Energy-Efficient Massive MIMO for Serving Multiple Federated Learning Groups

Tung T. Vu*, Hien Quoc Ngo*, Duy T. Ngo†, Minh N Dao‡, Erik G. Larsson§
*Institute of Electronics, Communications, and Information Technology (ECIT), Queen's University Belfast, Belfast BT3 9DT, UK
†School of Electrical Engineering and Computing, The University of Newcastle, Callaghan, NSW 2308, Australia
‡School of Engineering, Information Technology and Physical Sciences, Federation University, Ballarat, VIC 3353, Australia
§Department of Electrical Engineering (ISY), Linköping University, SE-581 83 Linköping, Sweden
Email: t.vu@qub.ac.uk, hien.ngo@qub.ac.uk, duy.ngo@newcastle.edu.au, m.dao@federation.edu.au, erik.g.larsson@liu.se

arXiv:2108.13512v2 [cs.IT] 17 Oct 2021

***Abstract*—With its privacy preservation and communication efficiency, federated learning (FL) has emerged as a learning framework that suits beyond 5G and towards 6G systems. This work looks into a future scenario in which there are multiple groups with different learning purposes and participating in different FL processes. We give energy-efficient solutions to demonstrate that this scenario can be realistic. First, to ensure a stable operation of multiple FL processes over wireless channels, we propose to use a massive multiple-input multiple-output network to support the local and global FL training updates, and let the iterations of these FL processes be executed within the same large-scale coherence time. Then, we develop asynchronous and synchronous transmission protocols where these iterations are asynchronously and synchronously executed, respectively, using the downlink unicasting and conventional uplink transmission schemes. Zero-forcing processing is utilized for both uplink and downlink transmissions. Finally, we propose an algorithm that optimally allocates power and computation resources to save energy at both base station and user sides, while guaranteeing a given maximum execution time threshold of each FL iteration. Compared to the baseline schemes, the proposed algorithm significantly reduces the energy consumption, especially when the number of base station antennas is large.**

I. Introduction

Recently, federated learning (FL) was introduced in [1] as an important step to bring machine learning closer to everyone. The breakthrough idea of FL is "no raw data sent to third party companies during learning processes", which means people can safely participate in FL processes without being worried that their personal data is exploited. A wide range of applications, such as healthcare and self-driving cars to name a few [2], [3], can benefit from FL. In FL, the learning is implemented jointly by many users (UEs). First, a local learning model is trained at each UE using local (private) training data, and sent to the central server. A global update is then computed at the central server using the local learning models transmitted from all UEs, and finally sent back to the UEs for local training updates. This learning process is iterated until reaching a certain learning accuracy level. To deploy the above iterative FL process over wireless networks, a key challenge is keeping the network energy consumption as low as possible. This is important both due to battery limitations of the UEs and to concerns about the ICT carbon footprint. It is thus critical to design an energy-efficient wireless network to support FL.

There are several studies of energy-efficient deployments of FL over wireless networks; see, e.g., [4]–[6] and references therein. In these works, the authors proposed designs which minimize the energy consumption at the UEs while guaranteeing the learning performance (i.e., the test accuracy) by jointly optimizing learning and communication parameters. However, the energy consumption of the transmission from the central server to the UEs was not taken into account. Also, these works proposed to use frequency-division multiple access (FDMA) and time-division multiple access (TDMA) systems to support FL. This might not be a good choice because FDMA and TDMA systems offer low UE data rates, and hence, yield a very high energy consumption, especially when the number of UEs is large. In addition, all these works only considered the case of a single FL group.

On the other hand, it is anticipated that the future wireless systems will need to serve multiple groups of UEs that participate in different FL processes. These networks need to simultaneously provide high data rates and high communication reliability to all UEs in all FL groups. Designing such networks is challenging and calls for a suitable, new wireless communication framework. To the best of our knowledge, there has not been any work studying energy-efficient wireless networks supporting multiple FL groups in the existing literature.

The contributions of this paper are summarized as follows:

- To support multiple FL groups over wireless networks, we propose using massive MIMO (mMIMO) and letting multiple iterations (each for one FL process of a group) be executed in one large-scale coherence time[1]. Thanks to the high array gain and multiplexing gain, mMIMO can simultaneously offer very high quality of service to all UEs in an area of interest [7], and hence, it is expected to guarantee a stable operation of each iteration (and hence the whole FL process).
- We introduce two specific transmission protocols where the steps within one FL iteration, i.e., the downlink transmission, the computation at the UEs, and the uplink transmission, are either asynchronous or synchronous. These schemes differ from the scheme in [8] which focuses on minimizing the training time of FL. Here, we use the unicast protocol on downlink and conventional multiuser transmission on uplink. Both downlink and uplink use zero-forcing (ZF) processing.
- We develop an algorithm to allocate the transmit powers

[1]The large-scale coherence time is defined as the time interval during which the large-scale fading coefficients remain approximately constant.

and processing frequencies to minimize the total energy consumption in each FL iteration, under a constraint on the total time taken for one FL iteration.

- Numerical results show that our proposed schemes significantly reduce the energy consumption compared to baseline schemes. They also confirm that the asynchronous scheme outperforms the synchronous scheme for supporting multiple FL groups, at the cost of a higher complexity.

II. Proposed Schemes and System Model

A. Multiple Federated Learning Framework

We consider a multiple FL network which includes multiple FL groups with different learning purposes. Each UE is assumed to only participate in one FL group. The FL frameworks of all groups can be different in terms of loss functions but have the same following four steps in each iteration [1], [9].

(S1) A central server sends a global update to the UEs.
(S2) Each UE updates and solves its local learning problem using its local data and then computes its local update.
(S3) Each UE sends its computed local update to the central server.
(S4) The central server computes the global update by aggregating the received local updates from all UEs.

The above process will be done iteratively until a certain learning accuracy level is achieved.

B. Proposed Schemes to Serve Multiple FL Groups

To support multiple FLs discussed in Section II-A, we propose to use mMIMO technology, i.e. Steps (S1) and (S3) of each FL iteration can be executed via the downlink and the uplink of a mMIMO system, respectively. Our proposed mMIMO-based multiple-FL system includes one M-antenna base station (BS) simultaneously serving N FL groups in the same frequency bands under the time-division-duplexing operation. We assume that the BS acts as the central server. Each FL iteration of each FL group is assumed to be executed within a large-scale coherence time, which is reasonable because the execution time of one FL iteration is smaller than the large-scale coherence time in many scenarios [8]. With this assumption, we then propose two specific transmission schemes to support the learning of N FL groups for each FL iteration as shown in Figs. 1(a) and (b) respectively.

(a) **Asynchronous scheme**: All groups start their FL iterations at the same time when the BS switches to a downlink mode. During this mode, BS simultaneously sends the global updates to all UEs in all groups (corresponding to Step (S1)). Each UE will start its local computation if it successfully receives the global training update (corresponding to Step (S2)). Then, the BS switches to an uplink mode immediately after the receptions of the global training update are completed at all the UEs. During this mode, the UEs will send their computed local updates to the BS (corresponding to Step (S3)) if they finish the local computation.

(b) **Synchronous scheme**: This scheme is similar to the asynchronous scheme except for the synchronization of Steps (S1)-(S3) among all the UEs. Each UE starts and waits for others to end each of those steps together.

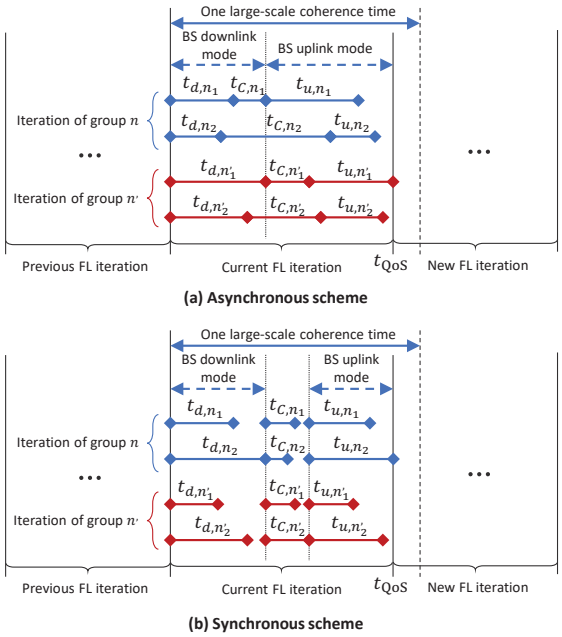


Fig. 1. Illustration of FL iterations over the considered mMIMO network with two groups n, n' and two UEs for each group

The time of one FL iteration under both schemes are constrained by a given period of time. Note that in the asynchronous scheme, the time of Steps (S1)–(S3) are optimally allocated (using the the proposed algorithm in the next section) to ensure that all the UEs finish one FL iteration and start a new FL iteration at the same time.

C. Massive-MIMO-based Multiple-FL System Model

The above two schemes share the common system model as follows. In each large-scale coherence time, the global and local updates in Steps (S1) and (S3) are transmitted in one or multiple small-scale coherence times depending on their sizes. Each coherence block in Step (S1) (or (S3)) involves the channel estimation phase and the downlink (or uplink) payload data phase. Suppose that at the considered time, there are N iterations of N FL groups being served. Let $\mathcal{N} \triangleq \{1, \ldots, N\}$, and $\mathcal{K}_n$ be the sets of groups and the indices of the UEs in group n, respectively. There are K_n single-antenna users (UEs) of each group n. The details of each step are presented in the following.

1) Step (S1): The BS sends the global updates to all UEs of all groups. Since the global updates intended for all UEs in a given group are the same, the transmission in this step corresponds to multi-group multicasting. Thus, we follow the scheme in [10] assuming orthogonal pilots and ZF processing.

Uplink channel estimation: For each coherence block of length τ_c, each UE sends its pilot of length $\tau_{d,p}$ to the BS [10]. We assume that the pilots of all the UEs are pairwisely orthogonal, which requires $\tau_{d,p} \geq K_{total} \triangleq \sum_{n \in \mathcal{N}} K_n$. Denote by $\boldsymbol{g}_{n_k} = (\beta_{n_k})^{1/2} \tilde{\boldsymbol{g}}_{n_k}$ the channel vector from UE k of group n to the BS, where β_{n_k} and $\tilde{\boldsymbol{g}}_{n_k}$ are the large-scale fading coefficient and small-scale fading coefficient vector,

respectively. At the BS, $\boldsymbol{g}_{n_k}$ is estimated by using the received pilots and the minimum mean-square error (MMSE) estimation technique. The MMSE estimate $\hat{\boldsymbol{g}}_{n_k}$ of $\boldsymbol{g}_{n_k}$ is distributed according to $\mathcal{CN}(\boldsymbol{0}, \hat{\sigma}^2_{n_k}\boldsymbol{I}_M)$, where $\hat{\sigma}^2_{n_k} = \frac{\tau_{d,p}\rho_p\beta^2_{n_k}}{\tau_{d,p}\rho_p\beta_{n_k}+1}$ [10]. We also denote by $\hat{\boldsymbol{G}} \triangleq [\hat{\boldsymbol{G}}_1, \ldots, \hat{\boldsymbol{G}}_N]$ the matrix stacking the channels of all the UEs, where $\hat{\boldsymbol{G}}_n \triangleq [\hat{\boldsymbol{g}}_{n_1}, \ldots, \hat{\boldsymbol{g}}_{n_{K_n}}]$.

Downlink payload data transmission: The BS encodes the global training update intended for UE k of group n into a symbol s_{d,n_k}, where $\mathbb{E}\{|s_{d,n_k}|^2\} = 1$, and apply the ZF precoding vector $\boldsymbol{u}_{n_k} = \sqrt{\eta_{n_k}\hat{\sigma}^2_{n_k}(M-K_{total})}\hat{\boldsymbol{G}}(\hat{\boldsymbol{G}}^H\hat{\boldsymbol{G}})^{-1}\boldsymbol{e}_{n_k,K_{total}}$ to precode the symbol, where η_{n_k} is a power control coefficient, $\boldsymbol{e}_{n_k,K_{total}}$ is the n_k-th column of $\boldsymbol{I}_{K_{total}}$, and $M \geq K_{total}$ is required. The transmitted signal at the BS is thus given as $\boldsymbol{x}_d = \sqrt{\rho_d}\sum_{n'\in\mathcal{N}}\sum_{\ell\in\mathcal{K}_{n'}}\boldsymbol{u}_{n'_\ell}s_{d,n'}$, where ρ_d is the maximum normalized transmit power at the BS. The transmitted power at the BS is required to meet the average normalized power constraint, i.e., $\mathbb{E}\{|x_d|^2\} \leq \rho_d$, which can be expressed through the following constraint:

$$\sum_{n\in\mathcal{N}}\sum_{k\in\mathcal{K}_n}\eta_{n_k} \leq 1. \tag{1}$$

The achievable rate $R_{d,n_k}(\boldsymbol{\eta})$ at UE k of group n is given as [10, (10)]

$$R_{d,n_k}(\boldsymbol{\eta}) = \frac{\tau_c - \tau_{d,p}}{\tau_c}B\log_2\left(1+\text{SINR}_{d,n_k}(\boldsymbol{\eta})\right), \tag{2}$$

where $\boldsymbol{\eta} \triangleq \{\eta_{n_k}\}_{n\in\mathcal{N},k\in\mathcal{K}_n}$, B is the bandwidth, and $\text{SINR}_{d,n_k}(\boldsymbol{\eta}) = \frac{(M-K_{total})\rho_d\hat{\sigma}^2_{n_k}\eta_{n_k}}{\rho_d(\beta_{n_k}-\hat{\sigma}^2_{n_k})\sum_{n'\in\mathcal{N}}\sum_{n'_\ell\in\mathcal{K}_{n'}}\eta_{n'_\ell}+1}$ is the effective downlink SINR[2].

Downlink delay: Let $S_{d,n}$ (bits) be the data size of the global training update of group n. The transmission time from the BS to UE k of group n is given by

$$t_{d,n_k}(\boldsymbol{\eta}) = \frac{S_{d,n}}{R_{d,n_k}(\boldsymbol{\eta})}.$$

Energy consumption for the downlink transmission: Denote by N_0 is the noise power. The energy consumption for transmitting the global update to the UE k of group n is the product of the transmit power $\rho_d N_0\eta_{n_k}$ and the delay for the downlink transmission to this UE. Therefore, the total energy consumption at the BS for all groups is

$$E_d(\boldsymbol{\eta}) = \sum_{n\in\mathcal{N}}\sum_{k\in\mathcal{K}_n}\rho_d N_0\eta_{n_k}t_{d,n_k}(\boldsymbol{\eta}) = \sum_{n\in\mathcal{N}}\sum_{k\in\mathcal{K}_n}\rho_d N_0\eta_{n_k}\frac{S_{d,n}}{R_{d,n_k}(\boldsymbol{\eta})}.$$

2) Step (S2): After receiving the global update, each UE executes L local computing rounds over its data set to compute its local update.

Local computation: Let c_{n_k} (cycles/sample) be the number of processing cycles for a UE k to process one data sample [9]. Denote by D_n (samples) and f_{n_k} (cycles/s) the size of the local data set and the processing frequency of the UE k of group n, respectively. The computation time at UE k of group n is then given by [8], [9]

$$t_{C,n_k}(f_{n_k}) = \frac{LD_nc_{n_k}}{f_{n_k}}.$$

Energy consumption for local computation at the UEs: The energy consumption at UE k of group n for computing its local training update is given as [8], [9]

$$E_{C,n_k}(f_{n_k}) = L\frac{\alpha}{2}c_{n_k}D_nf^2_{n_k},$$

where $\frac{\alpha}{2}$ is the effective capacitance coefficient of the UEs' computing chipset.

3) Step (S3): In this step, UEs' local updates are transmitted to the BS.

Uplink channel estimation: In each coherence block, each UE sends its pilot of length $\tau_{u,p}$ to the BS. We assume that the pilots of all the UEs are pairwisely orthogonal, which requires the pilots of length $\tau_{u,p} \geq K_{total}$. The MMSE estimate $\bar{\boldsymbol{g}}_{n_k}$ of $\boldsymbol{g}_{n_k}$ is distributed according to $\mathcal{CN}(\boldsymbol{0}, \bar{\sigma}^2_{n_k}\boldsymbol{I}_M)$, where $\bar{\sigma}^2_{n_k} = \frac{\tau_{u,p}\rho_p\beta^2_{n_k}}{\tau_{u,p}\rho_p\beta_{n_k}+1}$ [10].

Uplink payload data transmission: After computing the local update, UE k of group n encodes this update into symbols denoted by s_{u,n_k}, where $\mathbb{E}\{|s_{u,n_k}|^2\} = 1$, and sends baseband signal $x_{u,n_k} = \sqrt{\rho_u\zeta_{n_k}}s_{u,n_k}$ to the BS, where ρ_u is the maximum normalized transmit power at each UE and ζ_{n_k} is a power control coefficient. This signal is subjected to the average transmit power constraint, i.e., $\mathbb{E}\left\{|x_{u,n_k}|^2\right\} \leq \rho_u$, which is can be expressed in a per-UE constraint as

$$\zeta_{n_k} \leq 1, \forall n \in \mathcal{N}, n_k \in \mathcal{K}_n\,. \tag{3}$$

After receiving data from all UEs, the BS uses the estimate channels and ZF scheme to detect the UEs' message symbols. The ZF precoder requires $M \geq K_{total}$. The achievable rate (bps) of UE k in group n is given by [7, (3.28)]

$$R_{u,n_k}(\boldsymbol{\zeta}) = \frac{\tau_c - \tau_{u,p}}{\tau_c}B\log_2\left(1+\text{SINR}_{u,n_k}(\boldsymbol{\zeta})\right), \tag{4}$$

where $\text{SINR}_{u,n_k}(\boldsymbol{\zeta}) \triangleq \frac{(M-K_{total})\rho_u\bar{\sigma}^2_{n_k}\zeta_{n_k}}{\rho_u\sum_{n'\in\mathcal{N}}\sum_{n'_\ell\in\mathcal{K}_{n'}}(\beta_{n'_\ell}-\bar{\sigma}^2_{n'_\ell})\zeta_{n'_\ell}+1}$ is the effective uplink SINR.

Uplink delay: Denote by $S_{u,n}$ (bits) the data size of the local training update of group n. The transmission time from UE k of group n to the BS is given by

$$t_{u,n_k}(\boldsymbol{\zeta}) = \frac{S_{u,n}}{R_{u,n_k}(\boldsymbol{\zeta})}.$$

Energy consumption for the uplink transmission: The energy consumption for the uplink transmission at a UE is the product of the uplink power and the transmission time. In particular, the energy consumption at UE k of group n is given as [8], [9]

$$E_{u,n_k}(\boldsymbol{\zeta}) = \rho_u N_0\zeta_{n_k}t_{u,n_k}(\boldsymbol{\zeta}) = \frac{\rho_u N_0\zeta_{n_k}S_{u,n}}{R_{u,n_k}(\boldsymbol{\zeta})}.$$

Remark 1. *We obtain the achievable downlink and uplink rates in* (2) *and* (4)*, respectively, under the case that all users participate in the transmission. However, as shown from the two proposed schemes in Fig. 1, at a particular time, some UEs may have finished their transmission, and thus, do not participate in the downlink or uplink transmission with other UEs at the same time. This will not cause any issue with our design because the rates* (2) *and* (4) *are still always achievable under this case.*

[2]Although all the UEs of one group have the same encoded symbol, their achievable rates can be different (and hence, their transmissions do not finish simultaneously). This is feasible when using a code that sends a maximum number of parity bits corresponding to the UEs with the smallest SINR. Here, each UE will stop listening as soon as it successfully decodes its message. Thus, the UEs with higher SINRs can stop listening earlier than those with smaller SINRs.

4) Step (S4): After receiving all the local updates, the BS computes its global update. Since the computational capability of the central server is much more powerful than those of the UEs, the delay of computing the global update is negligible.

III. Problem Formulation and Solution

In practice, different groups are likely to start their FL processes at different times and have different number of FL iterations depending on their learning targets. Therefore, minimizing the energy consumption of the whole FL processes of all groups at the same time is tremendously difficult due to complicated synchronization among all groups. Instead, we aim at minimizing the total energy consumption in one FL iteration for all groups, which also leads to the total energy consumption reduction of the whole FL processes of all groups.

A. Asynchronous Scheme

The problem of minimizing the total energy consumption of one FL iteration for all groups is formulated as follows.

$$\min_{\boldsymbol{\eta},\boldsymbol{f},\boldsymbol{\zeta}} E_{total} \triangleq E_d(\boldsymbol{\eta}) + \sum_{n\in\mathcal{N}} \sum_{n_k\in\mathcal{K}_n} \left(E_{C,n_k}(f_{n_k}) + E_{u,n_k}(\boldsymbol{\zeta})\right) \quad (5a)$$

s.t. (1), (3)

$$0 \le \eta_n, 0 \le \zeta_{n_k}, \forall n, n_k \quad (5b)$$

$$0 \le f_{n_k} \le f_{\max}, \forall n, n_k \quad (5c)$$

$$t_{d,n_k}(\boldsymbol{\eta}) + t_{C,n_k}(f_{n_k}) + t_{u,n_k}(\boldsymbol{\zeta}) \le t_{\text{QoS}}, \forall n, n_k \quad (5d)$$

$$\max_{n\in\mathcal{N}} \max_{n_k\in\mathcal{K}_n} t_{d,n_k} \le \min_{n\in\mathcal{N}} \min_{n_k\in\mathcal{K}_n} \left(t_{d,n_k} + t_{C,n_k}\right), \quad (5e)$$

where $\boldsymbol{f} \triangleq \{f_{n_k}\}_{n\in\mathcal{N}, n_k\in\mathcal{K}_n}$. Here, (5d) guarantees the execution time of one FL iteration below a threshold t_{QoS} for maintaining the quality of service, and (5e) is introduced to ensure that all the UEs send their local update during the uplink mode of the BS. The right-hand side of (5e) models the first UE that finishes its downlink transmission and local computation, while the left-hand side presents the slowest UE finishes its downlink transmission as seen in Fig. 1(a).

To solve (5), we rewrite it in the following more tractable epigraph form

$$\min_{\boldsymbol{x}} \widetilde{E}_{total} \triangleq \sum_{n\in\mathcal{N}} \sum_{n_k\in\mathcal{K}_n} \rho_d N_0 S_{d,n} \omega_{n_k} + \sum_{n\in\mathcal{N}} \sum_{n_k\in\mathcal{K}_n} \left(L\frac{\alpha}{2} c_{n_k} D_n f_{n_k}^2 + \rho_u N_0 \theta_{n_k} S_{u,n}\right) \quad (6a)$$

s.t. (1), (3), (5b), (5c)

$$r_{d,n_k} \le R_{d,n_k}(\boldsymbol{\eta}), \forall n, n_k \quad (6b)$$

$$r_{u,n_k} \le R_{u,n_k}(\boldsymbol{\zeta}), \forall n, n_k \quad (6c)$$

$$0 \le r_{d,n_k}, 0 \le r_{u,n_k}, \forall n, n_k \quad (6d)$$

$$\eta_{n_k} \le r_{d,n_k}\omega_{n_k}, \forall n, n_k \quad (6e)$$

$$\zeta_{n_k} \le r_{u,n_k}\theta_{n_k}, \forall n, n_k \quad (6f)$$

$$\frac{S_{d,n}}{r_{d,n_k}} + \frac{LD_n c_{n_k}}{f_{n_k}} + \frac{S_{u,n}}{r_{u,n_k}} \le t_{\text{QoS}}, \forall n, n_k \quad (6g)$$

$$S_{d,n} \le r_{d,n_k} q, \forall n, n_k \quad (6h)$$

$$q \le q_{1,n_k} + q_{2,n_k}, \forall n, n_k \quad (6i)$$

$$0 \le q_{1,n_k}, 0 \le q_{2,n_k}, \forall n, n_k \quad (6j)$$

$$q_{1,n_k} r_{d,n_k} \le S_{d,n}, \forall n, n_k \quad (6k)$$

$$q_{2,n_k} f_{n_k} \le LD_n c_{n_k}, \forall n, n_k, \quad (6l)$$

where $\boldsymbol{x} \triangleq \{\boldsymbol{\eta}, \boldsymbol{f}, \boldsymbol{\zeta}, \boldsymbol{r}_d, \boldsymbol{r}_u, \boldsymbol{\omega}, \boldsymbol{\theta}, q, \boldsymbol{q}_1, \boldsymbol{q}_2\}$, $\boldsymbol{r}_d, \boldsymbol{r}_u, \boldsymbol{\omega}, \boldsymbol{\theta}, q, \boldsymbol{q}_1$, $\boldsymbol{q}_2$ are additional variables, $\boldsymbol{r}_d = \{r_{d,n_k}\}$, $\boldsymbol{r}_u = \{r_{u,n_k}\}$, $\boldsymbol{\omega} = \{\omega_{n_k}\}$, $\boldsymbol{\theta} = \{\theta_{n_k}\}$, $\boldsymbol{q}_1 = \{q_{1,n_k}\}$, $\boldsymbol{q}_2 = \{\boldsymbol{q}_{2,n_k}\}$, $\forall n \in \mathcal{N}, n_k \in \mathcal{K}_n$. Here, (6h)–(6l) come from (5e). If we let $\boldsymbol{v} \triangleq \{v_{n_k}\}$ and $\boldsymbol{u} \triangleq \{u_{n_k}\}, \forall n \in \mathcal{N}, n_k \in \mathcal{K}_n$, with $v_{n_k} \triangleq \eta_{n_k}^{1/2}$, $u_{n_k} \triangleq \zeta_{n_k}^{1/2}, \forall n, n_k$, then problem (6) will be equivalent to

$$\min_{\widetilde{\boldsymbol{x}}} \widetilde{E}_{total} \quad (7a)$$

s.t. (5c), (6d), (6g) − (6j)

$$r_{d,n_k} \le R_{d,n_k}(\boldsymbol{v}), \forall n, n_k \quad (7b)$$

$$r_{u,n_k} \le R_{u,n_k}(\boldsymbol{u}), \forall n, n_k \quad (7c)$$

$$v_{n_k}^2 - r_{d,n_k}\omega_{n_k} \le 0, \forall n, n_k \quad (7d)$$

$$u_{n_k}^2 - r_{u,n_k}\theta_{n_k} \le 0, \forall n, n_k \quad (7e)$$

$$\sum_{n\in\mathcal{N}} \sum_{k\in\mathcal{K}_n} v_{n_k}^2 \le 1 \quad (7f)$$

$$u_{n_k}^2 \le 1, \forall n, n_k \quad (7g)$$

$$0 \le v_{n_k}, 0 \le u_{n_k}, \forall n, n_k, \quad (7h)$$

$$q_{1,n_k} r_{d,n_k} - S_{d,n} \le 0, \forall n, n_k \quad (7i)$$

$$q_{2,n_k} f_{n_k} - LD_n c_{n_k} \le 0, \forall n, n_k, \quad (7j)$$

where $\widetilde{\boldsymbol{x}} \triangleq \{\boldsymbol{x}, \boldsymbol{v}, \boldsymbol{u}\} \setminus \{\boldsymbol{\eta}, \boldsymbol{\zeta}\}$. Here, (7d) and (7e) follow from (6e) and (6f), while (7f)–(7g) follow from (1), (3), and (5b). Problem (7) is still difficult to solve due to nonconvex constraints (7b), (7c), (7d), (7e), (7i), and (7j).

To deal with these constraints, we first observe that the rates $R_{d,n_k}(\boldsymbol{v})$ and $R_{u,n_k}(\boldsymbol{u})$ of nonconvex constraints (7b) and (7c) have the following concave lower bounds [11, (20)]:

$$\widetilde{R}_{d,n_k}(\boldsymbol{v}) \triangleq \frac{\tau_c - \tau_{cp}}{\tau_c \log 2} B\Big[\log\Big(1 + \frac{(\Upsilon_{n_k}^{(i)})^2}{\Pi_{n_k}^{(i)}}\Big) - \frac{(\Upsilon_{n_k}^{(i)})^2}{\Pi_{n_k}^{(i)}} + 2\frac{\Upsilon_{n_k}^{(i)}\Upsilon_{n_k}}{\Pi_{n_k}^{(i)}} - \frac{(\Upsilon_{n_k}^{(i)})^2(\Upsilon_{n_k}^2 + \Pi_{n_k})}{\Pi_{n_k}^{(i)}((\Upsilon_{n_k}^{(i)})^2 + \Pi_{n_k}^{(i)})}\Big] \le R_{d,n_k}(\boldsymbol{v}), \quad (8)$$

$$\widetilde{R}_{u,n_k}(\boldsymbol{u}) \triangleq \frac{\tau_c - \tau_{dp}}{\tau_c \log 2} B\Big[\log\Big(1 + \frac{(\Psi_{n_k}^{(i)})^2}{\Xi_{n_k}^{(i)}}\Big) - \frac{(\Psi_{n_k}^{(i)})^2}{\Xi_{n_k}^{(i)}} + 2\frac{\Psi_{n_k}^{(i)}\Psi_{n_k}}{\Xi_{n_k}^{(i)}} - \frac{(\Psi_{n_k}^{(i)})^2(\Psi_{n_k}^2 + \Xi_{n_k})}{\Xi_{n_k}^{(i)}((\Psi_{n_k}^{(i)})^2 + \Xi_{n_k}^{(i)})}\Big] \le R_{u,n_k}(\boldsymbol{u}), \quad (9)$$

where $\Pi_{n_k}(\boldsymbol{v}) = \rho_d(\beta_{n_k} - \hat{\sigma}_{n_k}^2)\sum_{n'\in\mathcal{N}}\sum_{n'_\ell\in\mathcal{K}_{n'}} v_{n'_\ell}^2 + 1$, $\Upsilon_{n_k}(v_{n_k}) = \sqrt{(M - K_{total})\rho_d}\hat{\sigma}_{n_k} v_{n_k}$, $\Xi_{n_k}(\boldsymbol{u}) = \rho_u \sum_{n'\in\mathcal{N}}\sum_{n'_\ell\in\mathcal{K}_{n'}}(\beta_{n'_\ell} - \bar{\sigma}_{n'_\ell}^2)u_{n'_\ell}^2 + 1$, and $\Psi_{n_k} = \sqrt{(M - K_{total})\rho_u}\bar{\sigma}_{n_k} u_{n_k}$. Next, the functions in the left-hand sides of constraints (7d), (7e), (7i), and (7j) have the following convex upper bounds [8]:

$$v_{n_k}^2 - r_{d,n_k}\omega_{n_k} \le h_{1,n_k}(v_{n_k}, r_{d,n_k}, \omega_{n_k}) \triangleq 0.25\big[4v_{n_k}^2 + (r_{d,n_k} - \omega_{n_k})^2 - 2(r_{d,n_k}^{(i)} + \omega_{n_k}^{(i)})(r_{d,n_k} + \omega_{n_k}) + (r_{d,n_k}^{(i)} + \omega_{n_k}^{(i)})^2\big], \quad (10)$$

$$u_{n_k}^2 - r_{u,n_k}\theta_{n_k} \le h_{2,n_k}(u_{n_k}, r_{u,n_k}, \theta_{n_k}) \triangleq 0.25\big[4u_{n_k}^2 + (r_{u,n_k} - \theta_{n_k})^2 - 2(r_{u,n_k}^{(i)} + \theta_{n_k}^{(i)})(r_{u,n_k} + \theta_{n_k}) + (r_{u,n_k}^{(i)} + \theta_{n_k}^{(i)})^2\big] \quad (11)$$

$$q_{1,n_k} r_{d,n_k} - S_{d,n} \le h_{3,n_k}(q_{1,n_k}, r_{d,n_k}) \triangleq 0.25\big[(q_{1,n_k} + r_{d,n_k})^2 - 2(q_{1,n_k}^{(i)} - r_{d,n_k}^{(i)})(q_{1,n_k} - r_{d,n_k}) + (q_{1,n_k}^{(i)} - r_{d,n_k}^{(i)})^2 - 4S_{d,n}\big] \quad (12)$$

Algorithm 1 Solving problem (5)

1: **Initialize**: Set $i=0$ and choose a random point $\widetilde{\boldsymbol{x}}^{(0)} \in \mathcal{F}$.
2: **repeat**
3: Update $i = i + 1$
4: Solving (20) to obtain its optimal solution $\widetilde{\boldsymbol{x}}^*$
5: Update $\widetilde{\boldsymbol{x}}^{(i)} = \widetilde{\boldsymbol{x}}^*$
6: **until** convergence

Output: $(\boldsymbol{\eta}^*, \boldsymbol{\zeta}^*, \boldsymbol{f}^*)$

$$q_{2,n_k} f_{n_k} - LD_n c_{n_k} \leq h_{4,n_k}(q_{2,n_k}, f_{n_k}) \triangleq 0.25\big[(q_{2,n_k} + f_{n_k})^2 - 2(q_{2,n_k}^{(i)} - f_{n_k}^{(i)})(q_{2,n_k} - f_{n_k}) + (q_{2,n_k}^{(i)} - f_{n_k}^{(i)})^2 - 4LD_n c_{n_k}\big]. \quad (13)$$

As such, constraints (7b), (7c), (7d), (7e), (7i), and (7j) can now be approximated respectively by the following convex constraints

$$r_{d,n_k} \leq \widetilde{R}_{d,n_k}(\boldsymbol{v}), \forall n, n_k \quad (14)$$

$$r_{u,n_k} \leq \widetilde{R}_{u,n_k}(\boldsymbol{u}), \forall n, n_k \quad (15)$$

$$h_{1,n_k}(v_{n_k}, r_{d,n_k}, \omega_{n_k}) \leq 0, \forall n, n_k \quad (16)$$

$$h_{2,n_k}(u_{n_k}, r_{u,n_k}, \theta_{n_k}) \leq 0, \forall n, n_k \quad (17)$$

$$h_3(q_{1,n_k}, r_{d,n_k}) \leq 0, \forall n, n_k \quad (18)$$

$$h_4(q_{2,n_k}, f_{n_k}) \leq 0, \forall n, n_k. \quad (19)$$

At iteration $(i+1)$, for a given point $\widetilde{\boldsymbol{x}}^{(i)}$, problem (6) can finally be approximated by the following convex problem:

$$\min_{\widetilde{\boldsymbol{x}} \in \widetilde{\mathcal{F}}} \widetilde{E}_{total}, \quad (20)$$

where $\widetilde{\mathcal{F}} \triangleq \{(5c), (6d), (6g) - (6j), (7f) - (7h), (14) - (19)\}$ is a convex feasible set.

In Algorithm 1, we outline the main steps to solve problem (5). Let $\mathcal{F} \triangleq \{(1), (3), (5b) - (5e)\}$ be the feasible set of (5). Starting from a random point $\widetilde{\boldsymbol{x}} \in \mathcal{F}$, we solve (20) to obtain its optimal solution $\widetilde{\boldsymbol{x}}^*$, and use $\widetilde{\boldsymbol{x}}^*$ as an initial point in the next iteration. The algorithm terminates when an accuracy level of ε is reached. In the case when $\widetilde{\mathcal{F}}$ satisfies Slater's constraint qualification condition, Alg. 1 will converges to a Karush-Kuhn-Tucker solution of (6) (hence (5)) [12, Theorem 1]. In contrast, Alg. 1 will converges to a Fritz John solution of (6) (hence (5)).

B. Synchronous Scheme

The optimization problem of this scheme is formulated as

$$\min_{\boldsymbol{\eta}, \boldsymbol{f}, \boldsymbol{\zeta}} E_d(\boldsymbol{\eta}) + \sum_{n \in \mathcal{K}_n} \sum_{k \in \mathcal{K}_n} (E_{C,n_k}(f_{n_k}) + E_{u,n_k}(\boldsymbol{\zeta})) \quad (21a)$$

$$\text{s.t. } (1), (3), (5b), (5c)$$

$$\max_{n \in \mathcal{N}} \max_{n_k \in \mathcal{K}_n} t_{d,n_k}(\boldsymbol{\eta}) + \max_{n \in \mathcal{N}} \max_{n_k \in \mathcal{K}_n} t_{C,n_k}(\boldsymbol{f}) + \max_{n \in \mathcal{N}} \max_{n_k \in \mathcal{K}_n} t_{u,n_k}(\boldsymbol{\zeta}) \leq t_{\text{QoS}}. \quad (21b)$$

Here, constraint (21b) captures the nature of "step-by-step", i.e., every UE needs to wait for the UEs of all groups to finish one step before starting the next step as seen in Fig. 1(b). Compared to (21b), (5d) provides more flexibility for allocating times of Steps (S1)–(S3) for each UE since the UEs do not need to wait for other UEs to start a new step.

Using the similar procedure to solve problem (5) above, we approximate (21) by the following convex problem

$$\min_{\widehat{\boldsymbol{x}}} \widetilde{E}_{total} \quad (22a)$$

$$\text{s.t. } (5c), (6d), (7f) - (7h), (14) - (17)$$

$$t_d + t_C + t_u \leq t_{\text{QoS}} \quad (22b)$$

$$\frac{S_{d,n}}{r_{d,n_k}} \leq t_d, \forall n, n_k \quad (22c)$$

$$\frac{LD_n c_{n_k}}{f_{n_k}} \leq t_C, \forall n, n_k \quad (22d)$$

$$\frac{S_{u,n}}{r_{u,n_k}} \leq t_u, \forall n, n_k, \quad (22e)$$

where $\boldsymbol{r}_d, \boldsymbol{r}_u, \boldsymbol{\omega}, \boldsymbol{\theta}, t_d, t_C, t_u$ are additional variables and $\widehat{\boldsymbol{x}} \triangleq \{\boldsymbol{v}, \boldsymbol{f}, \boldsymbol{u}, \boldsymbol{r}_d, \boldsymbol{r}_u, \boldsymbol{\omega}, \boldsymbol{\theta}, t_d, t_C, t_u\}$. Then, problem (21) can be solved using Algorithm 1 for iteratively solving (22).

C. Complexity Analysis

Problem (20) can be transformed to an equivalent problem that involves $V_1 \triangleq (9K_{total} + 1)$ real-valued scalar variables, $L_1 \triangleq (8K_{total} + 4)$ linear constraints, $Q_1 \triangleq 11K_{total}$ quadratic constraints. Therefore, problem (20) requires a complexitiy of $\mathcal{O}(\sqrt{L_1 + Q_1}(V_1 + L_1 + Q_1)V_1^2)$ [13]. The transformed version of problem (22) involves a smaller number of variables and constraints than the version of problem (20), i.e, $V_2 \triangleq (6K_{total} + 3)$ real-valued scalar variables, $L_2 \triangleq (6K_{total} + 1)$ linear constraints, $Q_2 \triangleq 5K_{total}$ quadratic constraints. Therefore, problem (22) has the complexity of $\mathcal{O}(\sqrt{L_2 + Q_2}(V_2 + L_2 + Q_2)V_2^2)$ which is lower than that of problem (20). As such, it is expected that the synchronous scheme requires a lower complexity than the asynchronous scheme. However, the synchronous scheme requires more signaling overhead to achieve synchronization than the asynchronous scheme.

IV. Numerical Examples

A. Network Setup and Parameter Setting

Consider a mMIMO network in a square of $D \times D$ km^2 where the BS is at the center and the UEs are randomly located. We set $\tau_c = 200$ samples. The large-scale fading coefficients, i.e., β_{mn_k}, are modeled in the same manner as [14, Eqs. (37), (38)]. For ease of presentation, we assume that all groups have the same number of UEs, i.e., $K_n = K, \forall n$. The total number of UEs is thus NK. We choose $\tau_{d,p} = \tau_{u,p} = NK$, $S_d = S_u =$ 20 MB, noise power $\sigma_0^2 = -92$ dBm, $L = 50$, $f_{\max} = 4 \times 10^9$ cycles/s, $D_n = 5 \times 10^6$ samples, $c_{n_k} = 20$ cycles/samples [9], for all n, n_k, $\alpha = 5 \times 10^{-30}$, $t_{\text{QoS}} = 5$ s. Let $\tilde{\rho}_d = 6$ W, $\tilde{\rho}_u = 0.2$ W and $\tilde{\rho}_p = 0.2$ W be the maximum transmit power of the APs, UEs and uplink pilot sequences, respectively. The maximum transmit powers ρ_d, ρ_u and ρ_p are normalized by the noise power.

B. Results and Discussions

Note that there are no other existing works studying wireless networks for supporting multiple FL groups. Therefore, to evaluate the effectiveness of our proposed asynchronous scheme (**OPT_Async**) and synchronous scheme (**OPT_Sync**), we consider the following heuristic schemes:

- **Heuristic_Async** (Heuristic solution for asynchronous scheme): The downlink power to the UEs of all groups are the same, i.e., $\eta_{n_k} = \frac{1}{NK}$ and the transmitted power of each UE is $\eta_{n_k} = 1, \forall n, n_k$. The processing frequencies are $f_{n_k} = \frac{LD_n c_{n_k}}{t_{\text{QoS}} - t_{d,n_k} - t_{u,n_k}}, \forall n, n_k$.

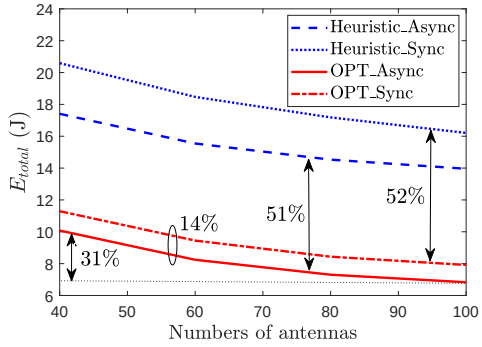


Fig. 2. Comparison among the proposed approach and baselines ($K = 10$ (users per group), $N = 3$ groups, $D = 0.25$ km).

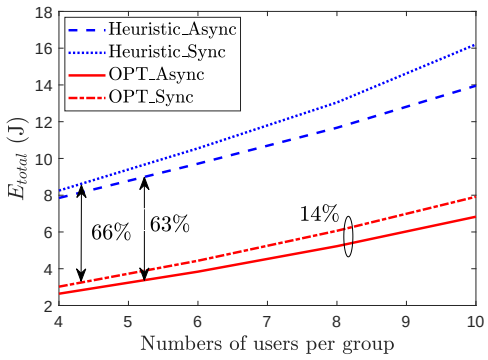


Fig. 3. Comparison among the proposed approach and baselines ($M = 100$ (antennas), $N = 3$ groups, $D = 0.25$ km).

- **Heuristic_Sync** (Heuristic solution for synchronous scheme): Similar to Heuristic_Async except for the processing frequencies which are set as $f_{n_k} = \frac{LD_n c_{n_k}}{t_{\text{QoS}} - \max_{n\in\mathcal{N}} \max_{n_k\in\mathcal{K}_n} t_{d,n_k} - \max_{n\in\mathcal{N}} \max_{n_k\in\mathcal{K}_n} t_{u,n_k}}, \forall n, n_k.$

Figs. 2 and 3 compare the total energy consumption of one FL iteration among the considered schemes. As seen, our proposed schemes give the best performance. Specifically, compared to heuristic schemes, the energy reduction are up to 52% with $M = 100$, $K = 10$, and up to 66% with $M = 100$, $K = 4$. The figures not only demonstrate the significant advantage of a joint allocation of power and processing frequency, but also show the benefit of using massive MIMO to support FL. Thanks to massive MIMO technology, the data rate of each UE increases when the number of antennas increases, leading to lower delays and then a decrease of 31% in the total energy consumption of one FL iteration as shown in Fig. 2.

Figs. 2 and 3 also shows that the asynchronous scheme slightly outperforms the synchronous scheme. In particular, the energy reduction in one FL iteration is up to only 14% with $M = 100$, $K = 10$. This is reasonable because the UEs in the asynchronous scheme do not need to wait for other UEs. As such, they have more time resource, and hence, can save more energy by using lower processing frequencies than those in the synchronous scheme. However, minimizing energy consumption results in maximizing the lowest data rate. Therefore, data rates obtained by the asynchronous scheme are relatively similar to those by the synchronous scheme, which leads to a similar performance of both schemes.

V. Conclusion

This work has proposed two novel schemes with mMIMO as energy-efficient solutions for future wireless networks to support multiple FL groups. Using successive convex approximation techniques, we have also successfully proposed an algorithm to allocate power and processing frequency in order to minimize the energy consumption in each FL iteration. Numerical results showed that our proposed schemes significantly reduces the energy consumption of each FL iteration compared to heuristic schemes. They also confirmed that in terms of energy savings, the asynchronous scheme is a better choice to support multiple FL groups than the synchronous scheme, though at the cost of higher complexity.

Acknowledgment

The work of T. T. Vu and H. Q. Ngo was supported by the U. K. Research and Innovation Future Leaders Fellowships under Grant MR/S017666/1. The work of Erik G. Larsson was supported in part by ELLIIT and the Knut and Alice Wallenberg Foundation. The work of Minh N. Dao was partially supported by Federation University Australia under Grant RGS21-8.

References

[1] B. McMahan *et al.*, "Communication-efficient learning of deep networks from decentralized data," in *Proc. Int. Conf. Artificial Intell. Stat. (AISTATS)*, Apr. 2017, pp. 1273–1282.

[2] Y. Chen *et al.*, "Fedhealth: A federated transfer learning framework for wearable healthcare," *IEEE Intell. Syst.*, vol. 35, no. 4, pp. 83–93, Aug. 2020.

[3] S. Niknam, H. S. Dhillon, and J. H. Reed, "Federated learning for wireless communications: Motivation, opportunities, and challenges," *IEEE Commun. Mag.*, vol. 58, no. 6, pp. 46–51, 2020.

[4] Z. Yang *et al.*, "Energy efficient federated learning over wireless communication networks," *IEEE Trans. Wireless Commun.*, vol. 20, no. 3, pp. 1935–1949, Mar. 2021.

[5] Q. Zeng, Y. Du, K. Huang, and K. K. Leung, "Energy-efficient radio resource allocation for federated edge learning," in *Proc. IEEE Int. Conf. Commun. Workshops (ICC Workshops)*, Jun. 2020, pp. 1–6.

[6] Y. Hu, H. Huang, and N. Yu, "Device scheduling for energy-efficient federated learning over wireless network based on TDMA mode," in *Proc. IEEE Int. Conf. Wireless Commun. Signal Process. (WCSP)*, Oct. 2020, pp. 286–291.

[7] T. L. Marzetta, E. G. Larsson, H. Yang, and H. Q. Ngo, *Fundamentals of Massive MIMO*. Cambridge University Press, 2016.

[8] T. T. Vu *et al.*, "Cell-free massive MIMO for wireless federated learning," *IEEE Trans. Wireless Commun.*, vol. 19, no. 10, pp. 6377–6392, Oct. 2020.

[9] N. H. Tran *et al.*, "Federated learning over wireless networks: Optimization model design and analysis," in *Proc. IEEE Conf. Comput. Commun. (INFOCOM)*, Apr. 2019, pp. 1387–1395.

[10] M. Sadeghi *et al.*, "Max–min fair transmit precoding for multi-group multicasting in massive MIMO," *IEEE Trans. Wireless Commun.*, vol. 17, no. 2, pp. 1358–1373, Feb. 2018.

[11] V. D. Nguyen *et al.*, "Spectral and energy efficiencies in full-duplex wireless information and power transfer," *IEEE Trans. Commun.*, vol. 65, no. 5, pp. 2220–2233, May 2017.

[12] B. R. Marks and G. P. Wright, "A general inner approximation algorithm for nonconvex mathematical programs," *Operations Research*, vol. 26, no. 4, pp. 681–683, Aug. 1978.

[13] H. H. M. Tam *et al.*, "Joint load balancing and interference management for small-cell heterogeneous networks with limited backhaul capacity," *IEEE Trans. Wireless Commun.*, vol. 16, no. 2, pp. 872–884, Feb. 2017.

[14] E. Björnson and L. Sanguinetti, "Making cell-free massive MIMO competitive with MMSE processing and centralized implementation," *IEEE Trans. Wireless Commun.*, vol. 19, no. 1, pp. 77–90, Jan. 2020.